High-Resolution Electron Energy Loss Spectroscopy Investigation of the Vibrational Structure and Order of an Octadecanethiol Monolayer on Gold Substrates

A.-S. Duwez,* L.-M. Yu, J. Riga, J. Delhalle, and J.-J. Pireaux

Laboratoire Interdisciplinaire de Spectroscopie Electronique, Facultés Universitaires Notre-Dame de la Paix, rue de Bruxelles 61, 5000 Namur, Belgium

Received: November 5, 1999; In Final Form: June 19, 2000

The vibrational spectra induced by electron beam from octadecanethiol monolayers adsorbed on gold are reported as a contribution to study in detail the structure of the layers, through an analysis of the interaction mechanisms between the electrons and these organic ultrathin films. To show the different spatial distribution of scattered electrons from dipole and impact interactions with the monolayer, angular distributions of elastic and inelastic scattered electrons were measured for various primary energies. The absolute electron scattering loss probabilities from both dipole and impact interactions were estimated for different vibrational modes. The study of these different mechanisms was first hampered by the poor order of the layers adsorbed on evaporated gold. It became therefore highly desirable to perform the experiments on a single-crystal substrate. Using Au(111) and Au(100) single crystals as substrates, it was possible to separate the spectral response from impact and dipole interacting electrons. A negative ion resonant behavior has been observed in the energy dependence of the electron scattering differential cross sections.

1. Introduction

This high-resolution electron energy loss spectroscopy (HREELS) investigation is reported as a contribution to a general effort to assess the potential of electron spectroscopies to elucidate the molecular structure of organic surfaces. In the past 10 years, there has been keen interest in using this spectroscopy for studying the surfaces of molecular solids and organic films.[1−14] In this specific application, the quantitative understanding of the interaction between low-energy electrons and the investigated surface is still an open question. Using an electron beam of low energy, HREELS has intrinsically a great sensitivity to the extreme surface and can evidence vibrational excitations at lower energy than infrared spectroscopy. By selecting appropriate experimental conditions, HREELS can access information about electronic transitions or vibrational properties of adsorbed molecules. All vibrational modes (infrared as well as Raman active and optically silent modes) can be observed in the spectra.[15]

The principle of this method consists of irradiating a surface with a monokinetic well-collimated electron beam and measuring the intensity of backscattered electrons, in a given direction, as a function of the energy loss transferred to the material surface. The resulting electron energy distribution curve contains features specific to each characteristic value of the final energy of the scattered electrons. Electrons that do not undergo any loss are detected as an elastic peak.

When low-energy electrons approach a solid surface, they can be scattered by three principal mechanisms: dipole, impact, and resonance scattering. The relative importance of these different interactions depends essentially on the primary energy of the electrons and the geometry of analysis. In the case of a dipole scattering process,[15] the primary electron interacts via long-range Coulomb forces with the dipole field associated with elementary excitations of the sample surface (phonons, plasmons, excitons, molecular vibrations, etc.). This implies that only modes for which the dipole moment changes during the vibration can be excited. This is the same selection rule as for the detection of active modes in infrared spectroscopy. The long-range nature of the Coulomb potential implies that the probing electrons interact preferentially with long wavelength quanta. As a small momentum transfer accompanies the excitation, the electrons are scattered into a narrow lobe near the specular direction. The dipole active modes are thus expected to determine the energy loss spectrum recorded in the specular geometry. The cross section for dipole scattering increases for decreasing primary energy, following an E^{-1} law for vibrations of adsorbed molecules on a metallic substrate.

In the impact scattering mechanism,[15−17] the primary electrons are inelastically scattered by the local atomic potentials of the solid surface, i.e. individual atoms or molecules. This short-range interaction involves large momentum transfers. The scattered electrons are thus distributed inside a broad angular lobe. The cross section for impact scattering increases with increasing E_p. Selection rules exist but allow almost all vibrations to be excited by this mechanism. Consequently, HREELS is a complementary technique to infrared spectroscopy. Moreover, impact scattering is extremely surface sensitive as the electron mean free path in the sample determines the probe depth.

Resonance scattering[18] results from the trapping of a primary electron in a vacant orbital of an atom or a molecule at the surface. This is a particular case of the short-range impact interaction. It arises when the energy of the incident electrons matches the energy of an empty level of the solid. The resulting negatively charged excited state of the atom is characterized by a rather short lifetime (10^{-10}−10^{-15} s) and its de-excitation process can lead to a vibrationally excited final state.

Each of these interaction mechanisms presents a characteristic property.[15] The angular distribution of dipole scattered electrons

* To whom correspondence should be addressed. Current address: Unité de Physique et de Chimie des Hauts Polymères, Université Catholique de Louvain, Place Croix du Sud, 1, B-1348 Louvain-La-Neuve, Belgium.

10.1021/jp993935e CCC: $19.00
Published on Web 08/24/2000

is very sharp in the specular direction, while, for impact excitation, a rather smooth variation of the signal intensity is observed over a wide angular range. The angular analysis of the intensity of the scattered electrons allows easy (in principle) identification of the dipole interacting electrons. It is very interesting to apply this knowledge to the study of very well organized thin films, as there are very few references dealing with this subject for organic/polymer layers (see, for example, refs 1−12). Notably, Wandass and Gardella[3−5] reported the first HREELS spectra of Langmuir−Blodgett monolayers of fatty acids on polycrystalline substrates. They evidenced a complex relationship between the character of the observed spectra and the nature of the substrate.

With the purpose of investigating the vibrational spectra of organic films induced by electron beam, we consider here self-assembled monolayers of alkanethiols on gold, which from their well-defined composition, thickness, and molecular structure[19−20] provide particularly well-suited reference samples.

2. Experimental Details

2.1. Materials. Gold substrates were prepared by evaporating gold (∼1000 Å) onto silicon wafers (100) following the procedure described elsewhere.[21] Postdeposition thermal treatment (annealing) of gold-coated slides was carried out in air, at 250 °C for 180 min (10°/min). The obtained substrates are polycrystalline with a (111) preferential orientation, and a typical grain size of about 1000 Å. Gold(111) and -(100) single crystals were lent by R. Feidenhans'l (Risø National Laboratory, Denmark). Octadecanethiol (Aldrich 98%) was used as received.

Preparation of Monolayers. Prior to their use, the gold substrates were cleaned to ensure a good adsorption of the thiols. The Au/Si slides were freed from contaminants by oxygen plasma treatment, and the treated Au slides were then immersed in ethanol to remove the gold oxide before monolayer assembly.[22] The gold single crystals were cleaned in ultrahigh vacuum (UHV) by repeated cycles of argon sputtering and annealing until a characteristic LEED pattern was obtained. Adsorption proceeded then by immersing the gold substrates for 2 or 18 h in 10^{-3} M solutions of alkanethiols, using absolute ethanol as a solvent. Upon removal from the solution, the samples were rinsed twice with *n*-hexane and absolute ethanol and dried in an argon stream.

2.2. Quality of Monolayers. The atomic C/S ratios, obtained from the area of the photoemission peaks corresponding to the C1s and S2p levels, were close to the expected theoretical values. These ratios have been obtained from X-ray photoemission spectra (XPS) recorded with a Scienta ESCA-300 spectrometer using the (Al $K\alpha_{1,2}$) monochromatized radiation (1486.6 eV). The TOA was 90°. No oxygen contamination could be found in these spectra. The monolayers have also been characterized by contact angles measurements, ellipsometry, IRAS, electrochemical measurements, UPS, and photoemission with synchrotron radiation, the results of which are presented elsewhere.[23−25]

2.3. HREELS Measurements. The spectra were recorded using an UHV vessel containing a 180° hemispherical monochromator and analyzer ensemble (SEDRA ISA RIBER), described in detail elsewhere.[8] The instrumental contribution to the resolution for the energy range used in this work was about 8 meV. All the spectra have been normalized to the total area under the spectrum. As an indication, typical counting rates are on the order of 70 000 counts s^{-1} for a monolayer adsorbed on a Au(111) single crystal and 4000 counts s^{-1} for a monolayer adsorbed on a Au/Si substrate.

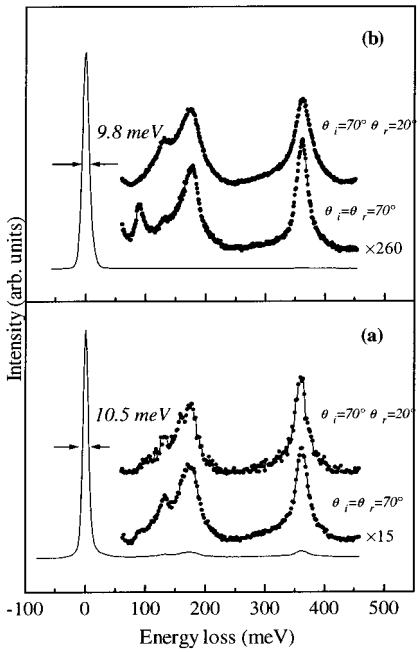

Figure 1. Specular ($\theta_i = \theta_r = 70°$) and off-specular ($\theta_i = 70°$, $\theta_r = 20°$) energy loss spectra of an octadecanethiol monolayer adsorbed on a Au/Si substrate (a) and on a Au(111) single crystal (b). The primary energy is 4 eV.

3. Results and Discussion

The vibrational spectrum of an octadecanethiol monolayer adsorbed on a Au/Si substrate and on a Au(111) single crystal (Figure 1) has been recorded in the specular and in the off-specular direction with an electron beam of 4.0 eV. The high and broad peak centered around 360 meV is associated with the C−H symmetric and antisymmetric stretching modes of the methylene groups, observed respectively at 2850 and 2920 cm^{-1} in the infrared spectroscopy (1 meV ≅ 8.1 cm^{-1}). This peak includes also the CH_3 symmetric and antisymmetric stretching modes (2879, 2937, and 2965 cm^{-1}), but all these components are not detectable in the HREELS spectra, the resolution being not good enough (∼10 meV, 81 cm^{-1}). The band appearing at 180 meV (1460 cm^{-1}) can be attributed to the scissoring mode of the CH_2 units of the chain and also to the CH_3 symmetric bending mode, which is situated around the same energy. The peak at 132 meV (1060 cm^{-1}) corresponds to the frequency of the C−C stretching mode of the carbon skeleton. Finally, around 90 meV (720 cm^{-1}), a peak is found corresponding to the vibrational frequency of the rocking mode of the CH_2.

The shoulder that appears between 30 and 40 meV (Figure 2) can be attributed to the Au−S stretching mode. This vibration has already been observed at 30 meV by Nuzzo et al. in the HREELS spectrum of methanethiol and dimethyl disulfide monolayers on gold[26] and around 37 meV by Stern et al. on thiophenol films on Pt(111).[27]

3.1. Angular Distribution of Scattered Electrons: Order of the Monolayer on Different Substrates. The specular ($\theta_i = \theta_r = 70°$) and off-specular ($\theta_i = 70°$, $\theta_r = 20°$) spectra from an octadecanethiol monolayer adsorbed on Au/Si substrates are very similar (Figure 1a). We chose an incident angle of 70°, more grazing than the angle of 45° usually used, to increase the interaction time between the electric field of the probe electrons and the surface, and thus also the dipole contribution. The angular distribution of the elastic peak from this monolayer is very broad ($\Delta\theta \cong 20°$), nearly purely impact-like. From these observations, we conclude that the octadecanethiol films on Au/

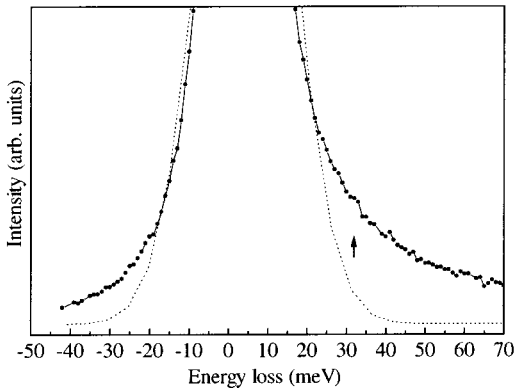

Figure 2. Specular ($\theta_i = \theta_r = 45°$) energy loss spectra in the elastic peak region recorded from an octadecanethiol monolayer adsorbed on a Au/Si substrate. The primary energy is 4 eV.

Si substrates are not highly ordered. The poor order of the layers hampers the study of the interaction mechanisms between the electrons and the samples. HREELS spectra are indeed highly sensitive to the ordering of the samples: regarding the elastic scattering, the surface will produce sharp Bragg-reflected beams (observed by low-energy electron diffraction, LEED) if it has a crystalline order and a diffuse intensity distribution if it has a disordered structure.[28] In the latter case, even the elastic electrons are scattered quasi-isotropically in all directions inside a broad solid angle, so the HREELS spectrum becomes essentially insensitive to the scattering direction. In an attempt to improve the ordering of these films, we adsorbed them on Au(111) and on Au(100) single crystals. The typical spectral resolution obtained on these samples was about 9−10 meV. The specular and off-specular spectra are shown in Figure 1b in the case of the Au(111) substrate. The spectral features are clearly different according to the reflection angle. Please note that the magnification scale factors in spectra a and b are related to the sample order, too. The absolute counting rate of the elastic peak in the specular spectrum is much larger (17 times) for the layer adsorbed on the single crystal than on the Au/Si substrate; this is also an indication of a better ordering. The electrons reflected by a dipole mechanism are indeed scattered in a sharp lobe around the specular direction, whereas the same quantity of electrons is diffused in a broader solid angle when interacting with a disordered sample. The spectra recorded from the layer adsorbed on Au(100) give similar results. The angular width ($\Delta\theta$) of the elastic peak is about 2.8° for the monolayer adsorbed on the Au(111) single crystal and about 5.3° for the monolayer adsorbed on the Au(100) single crystal, whereas it is about 20° in the case of the Au/Si substrate. The $\Delta\theta$ are thus smaller when the layer is adsorbed on Au(111), suggesting that the octadecanethiol film is more ordered on Au(111) than on Au(100). If the coherent domains are supposed to be circular, a rough estimation of their diameter (D) can be obtained from the angular width $\Delta\theta$ (rd) of the elastic peak:[28]

$$D = \frac{\lambda}{2\Delta\theta\cos\theta}$$

where λ is the de Broglie wavelength associated with the incident electrons of energy E_p (in eV),

$$\lambda = \frac{12.2}{\sqrt{E_p}}$$

and θ is the angle of incidence.

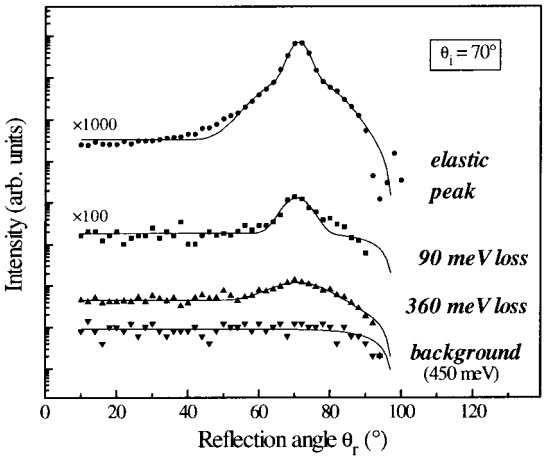

Figure 3. Angular distribution curves of the elastic peak intensity, of the 90 and the 360 meV losses, and of the background (at 450 meV), recorded from an octadecanethiol monolayer on Au(111). The primary energy is 1 eV and the angle of incidence is 70°. The full lines are fits to the data and are used as a guide to the eye. Please note the vertical log scale.

Since the intrinsic angular dispersion of the primary electron beam is about 1.2°, the broadening of the elastic line amounts to $\Delta\theta = 2.8 - 1.2 = 1.6°$ ($1.6° \cong 0.028$ rd) for a primary energy of 4 eV in the case of the Au(111) substrate and amounts to $\Delta\theta = 5.3 - 1.2 = 4.1°$ in the case of the Au(100) substrate. Inserting these values into the above equation yields then domain sizes of about 320 and 125 Å, respectively. The difference in domain size shows that the substrate crystallography strongly influences the packing and the organization of the monolayer. Strong and Whitesides have indeed shown that the symmetry of sulfur atoms on Au(111) is hexagonal and is a based centered-square on Au(100).[29] Scanning probe microscopy results from the literature (and particularly STM experiments)[30,31] are consistent with the calculated domain sizes based upon HREELS angular dispersions. For example, domain sizes measured by STM on Au(111) vary usually between 200 and 400 Å.[30,31]

3.2. Dipole and Impact Contribution in the HREELS Spectra of an Octadecanethiol Monolayer on Au(111). To evidence and separate dipole and impact processes, angular distributions of elastically and inelastically scattered electrons were measured, for various primary energies at an incident angle of 70°. As a typical result, the angular profile of the elastic peak intensity measured around the specular direction for a primary energy of 1.0 eV from the octadecanethiol film adsorbed on Au(111) is shown in Figure 3. A sharp lobe appears in the specular direction ($\theta_i = \theta_r = 70°$), underpinned by a broad background, which can be understood as the result of a mixture between dipole and impact scattering.

As is well-known, the off-specular spectra are dominated by the electrons interacting by an impact mechanism, but they also contain a small quantity of electrons from the dipole scattering by the disordered molecules (diffuse scattering). Similarly, we can also be convinced that, in the specular direction, a small fraction of the analyzed electrons are impact-scattered. HREELS off-specular spectra are shown in Figure 4a. The intensity ratio between the impact spectra in the specular and off-specular direction can be determined by measuring the ratio of the background intensities (around 450 meV energy loss) at specular and off-specular angles. Multiplying the off-specular spectra by this ratio, we were able to extrapolate the impact HREELS spectra in the specular direction.[11] One example is shown in Figure 5. In panel a, the full line is the scaled off-specular spectrum ($\theta_r = 20°$), representing the impact contribution in

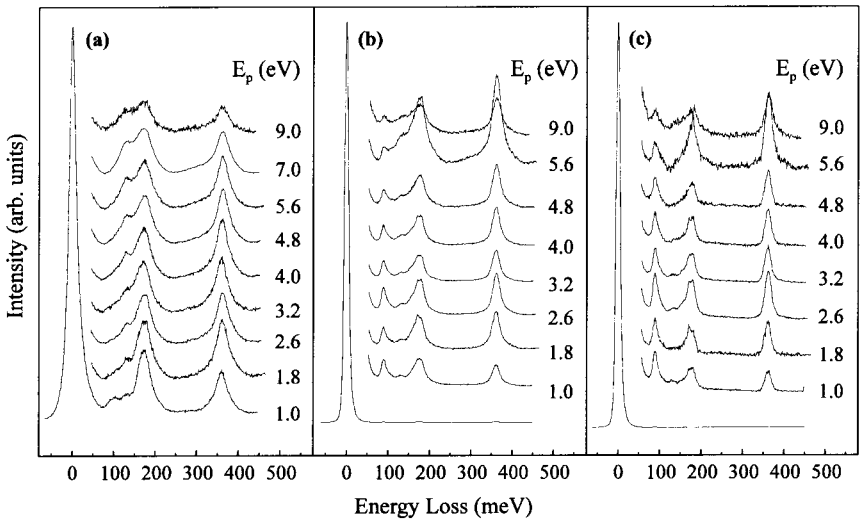

Figure 4. Off-specular ($\theta_i = 70°$, $\theta_r = 20°$) (a), specular ($\theta_i = \theta_r = 70°$) (b), and "pure dipole" spectra (c) of an octadecanethiol monolayer adsorbed on a Au(111) single crystal, at different primary energies.

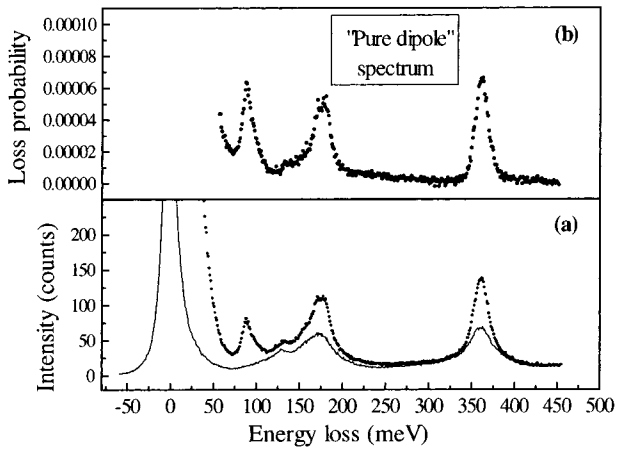

Figure 5. (a) Specular spectrum (dots) and scaled off-specular spectrum (full line), representing the impact contribution in the specular direction. The spectra were recorded from an octadecanethiol monolayer on Au(111) with a primary energy of 4 eV and an incident angle of 70°. (b) "Pure dipole" spectrum obtained by subtracting the two spectra plotted in panel a and then by normalizing to the total area under the spectrum.

the specular direction, and the dots represent the corresponding experimental specular spectrum ($\theta_r = 70°$). By subtracting the impact spectral contribution from the specular spectrum (i.e. by subtracting the two spectra plotted in panel a), the "pure dipole" scattering spectrum of the monolayer is obtained (Figure 5b and Figure 4c).

The pure dipole spectra are rather similar to the infrared spectrum of polyethylene, whereas the off-specular spectra are similar to its Raman spectrum.[13] So, this is a clear validation of the data handling method. It is thus possible to extract the spectral response of infrared active vibrations from the specular spectra. Our dipole spectra are also similar to the HREELS spectrum obtained by Apai et al.[13] from polyethylene thin films with a primary energy lower than (or equal to) 3 eV, and our off-specular spectra are similar to the HREELS polyethylene spectrum recorded with a primary energy higher than 5 eV. At low incident energy, the HREELS spectra are indeed dominated by dipole excited modes, and when the incident electron energy is increasing, the impact interaction mechanism becomes predominant. The ensemble of spectra in Figure 4c shows, however, that it is possible for any incident energy to extract from the recorded HREELS spectra the "pure dipole" contribution, without any impact contamination. The identification of the peaks observed in the off-specular and the "pure dipole" spectra is summarized in Table 1.

TABLE 1: Position of the Peaks (meV) Observed in Parts a (off-specular spectra) and c ("pure dipole" spectra) of Figure 4 and Their Assignment

	off-specular spectra	pure dipole spectra
C-H stretching	362	362
CH_2 scissoring and CH_3 bending	180	180
CH_2 wagging	162	162
C-C stretching	130	not visible
CH_2 rocking	only visible for $E_p = 1.0$ eV	90 very intense

3.3. Excitation Probability of Molecular Vibrations. From the spectra in Figure 4 and from Table 1, it is very likely that the rocking mode of CH_2 (90 meV) is excited preferably by a dipole mechanism, since it is enhanced in the specular and pure dipole spectra. The C−C stretching vibrations appear excited by an impact mechanism, as the corresponding peak (132 meV) is more visible in the off-specular spectra and, moreover, its intensity increases with the primary energy. No evident conclusion can be drawn from the behavior of the C−H bending and stretching vibrations.

To accurately discuss the evolution of the intensities and thus to provide more insight in the understanding of the interactions between electrons and monolayers, the absolute electron scattering loss probability for both dipole and impact interactions can be estimated from the different loss intensities (which have been normalized to the spectrum area, i.e. to the total number of the scattered electrons) versus the primary energies. The intensity of four losses has been measured in the pure dipole and the off-specular spectra. The data are presented in parts a and b of Figure 6, respectively.

The most intense peak in the pure dipole spectrum at low primary energy (Figure 6a) is the rocking mode of CH_2 at 90 meV. Its intensity decreases with increasing primary energies; that is the typical behavior of a dipole mode. The C−C stretching mode has a low loss probability that is slightly increasing for higher incident energies, revealing an impact interaction mechanism. The loss probability from the scissoring and bending mode does not present an evolution typical either of an impact or of a dipole interaction. The behavior of the stretching vibration versus the primary energy is typical of an

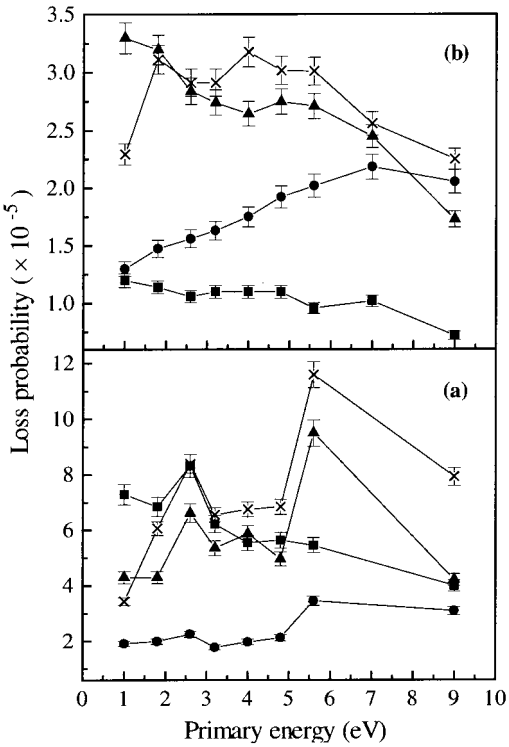

Figure 6. Loss probabilities of the vibrational modes detected in the "pure dipole" spectra (a) and in the off-specular spectra (b) of an octadecanethiol monolayer on Au(111) versus the primary energy of the electrons: ■, CH_2 rocking (90 meV); ●, C−C stretching (130 meV); ▲, CH_2 scissoring and CH_3 bending (180 meV), ×, CH_2 and CH_3 stretching (360 meV).

impact interaction. Almost all the losses handled at Figure 6a present an abrupt increase in intensity at about 2.6 and 5.6 eV. This enhancement is characteristic of a resonance phenomenon.[18] The resonance structure at 5.6 eV is well-known. Previous studies have shown the existence of such a resonance around 8 eV for methane in the gas phase,[14,32] around 5.5 eV for the C−H stretching band of organic films,[5,9] and at 6.0 eV for a hexatriacontane film.[33] On the contrary, the resonance structure at 2.6 eV has never been observed before in the case of hydrocarbon molecules. It might thus come from modifications in the electronic structure of the alkane chain due to additional unoccupied states resulting from the presence of the sulfur moiety. To identify the level on which the electron is trapped during the resonance mechanism, the unoccupied electronic states of the molecule have to be known, for instance, from theoretical calculations, inverse photoemission, or EELS studies. Unfortunately, the inverse photoemission measurements are not realizable on our samples since the electron beam usually used in these experiments produces a high current ($\sim 10^{-6}$ A) which will destroy the monolayers, as it is often the case in LEED experiments.[34] Studies of electronic transitions by EELS are now underway.

In the off-specular loss probability plot (Figure 6b), the intensity of the CH_2 rocking mode is very weak and decreases when the incident energy is increasing, confirming the dipole interaction evidenced above. The C−C stretching mode comes clearly from an impact interaction, as evidenced from its rising intensity. The CH_2 scissoring and CH_3 bending modes are probably excited by a dipole interaction, as shown by their decreasing intensity. The dipolar behavior of the losses at 90 and 160 meV in the off-specular spectra comes probably from the dipole interaction between electrons and the disordered molecules, producing a diffuse intensity distribution. The cross section curve of the CH_2 and CH_3 stretching vibrations has a particular shape: it increases between 1 and 5 eV and decreases for higher primary energies. Such a shape is again characteristic of a resonance phenomenon (see above). The width of this resonance structure, centered on 5 eV, is about 6 eV. The width of a resonance peak being linked to the lifetime of the resonance state by the Heisenberg incertitude principle, we may estimate that the de-excitation process occurs rapidly ($\sim 1 \cdot 10^{-16}$ s).

As a summary, the rocking mode of CH_2 as well as the CH_2 scissoring and CH_3 bending modes seem thus to be preferentially excited by a dipole mechanism, whereas the stretching modes of C−C and C−H are excited preferentially by an impact mechanism.

In addition to these observations, we paid particular attention to the angular distributions of the losses at 90 and 360 meV (C−H rocking and stretching modes). We have measured the intensity of these peaks versus the angle of analysis away from the specular direction ($\theta_i = 70°$) for primary energies of 1 (Figure 3) and 4 eV. From inspection of Figure 3, we note that the 90 meV loss has an angular profile rather similar to the one of the elastic peak, whereas the 360 meV loss has an angular shape closer to the background profile (measured at 450 meV) coming from the impact interaction. For an incident energy of 1 eV, the full angular width at half-maximum (fwhm) of the elastic line is 5.6° and the 90 meV structure is only 0.3° broader. This confirms our previous conclusion that the rocking vibrational mode is excited by a dipole mechanism. On the contrary, the 360 meV peak has a much broader, nearly purely impact-like angular distribution shape, confirming also the previous observations.

By varying the incident angle of the electrons, the contribution of the dipole interaction in the energy loss spectra can be modified. A high value of θ_i (corresponding to a more grazing incident angle) increases the interaction time between the electrons and the vibrations, increasing thus the dipole interaction probability. Figure 7a,b shows the specular and "pure dipole" spectra recorded from the octadecanethiol monolayer on Au(111) with a primary energy of 3 eV and for different incident angles. The rocking mode of CH_2 (90 meV), which is excited by a dipole mechanism as discussed above, is clearly enhanced at more grazing angles, whereas the C−C stretching mode (130 meV), which was shown to be excited by an impact mechanism, is more visible at a lower angle (i.e. closer to the normal incidence). The intensities of the vibrational modes detected in Figure 7b have been reported as a function of the incident angle (Figure 8a). The loss probability increases with the incident angle, except for the C−C stretching mode, for which the loss probability is higher at lower angles. The dipolar contribution to the interaction between electrons and C−H rocking, stretching, and scissoring (or bending) vibrational modes is thus clearly enhanced at grazing angles. The off-specular spectra recorded at different incident angles are shown in Figure 7c and the corresponding peak intensities are plotted in Figure 8b as a function of the incident angle. No important variation of the loss probabilities is observed from Figure 8b. Only the C−H stretching mode seems to be slightly enhanced at $\theta_i = 40°$. The incident angle of the incoming electrons has no significant influence in the off-specular spectral features.

4. Conclusions

The comparison between specular and off-specular HREELS spectra has evidenced the poorly ordered structure of all the films deposited on gold-coated silicon and it was thus impossible to distinguish between the impact and dipolar spectral contribu-

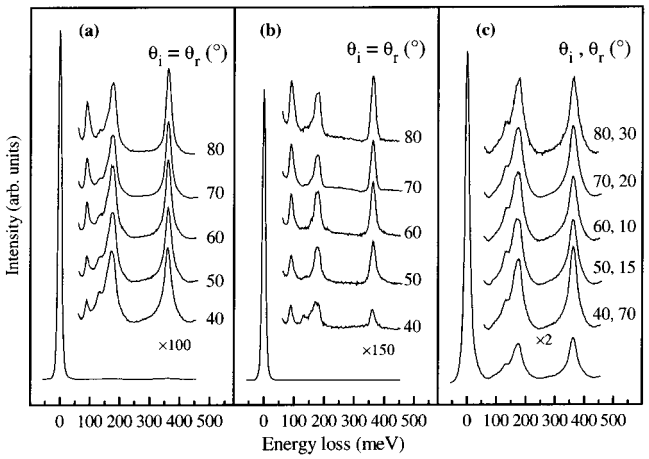

Figure 7. Specular (a), "pure dipole" (b), and off-specular (c) spectra of an octadecanethiol monolayer adsorbed on a Au(111) single crystal, recorded with a primary energy of 3 eV and at different incident angles.

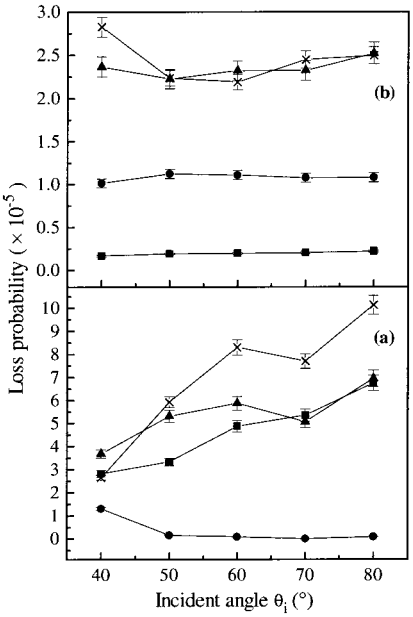

Figure 8. Loss probabilities of the vibrational modes detected in the "pure dipole" spectra (a) and in the off-specular spectra (b) of an octadecanethiol monolayer on Au(111) versus the incident angle of the electron beam (The primary energy is 3 eV.): ■, CH_2 rocking (90 meV); ●, C−C stretching (130 meV); ▲, CH_2 scissoring and CH_3 bending (180 meV); ×, CH_2 and CH_3 stretching (360 meV).

tions. The angular distribution of the elastic peak was very broad, nearly purely impact-like. Performing the experiment on a gold single crystal improved considerably the order in the monolayers. We were thus able to study in detail the different interaction mechanisms between the electrons and the layers and to determine the preferential mechanism for each vibration. We have extrapolated the impact spectrum in the specular direction and, subtracting this impact contribution from the specular spectrum, we have obtained an estimation of the "pure dipole" scattering spectrum of the monolayer. The electron scattering loss probability for both dipole and impact interactions have been estimated from the different loss intensities versus the primary energies. It has been shown that the rocking and scissoring modes of CH_2 and the CH_3 bending modes are preferentially excited by a dipole mechanism, whereas the C−C and C−H stretching modes are excited preferentially by an impact mechanism. The dipole contribution in the energy loss spectra can be modified by varying the incident angle of the electron beam.

The surface ordering of these monolayers is thus mainly governed by the lattice matching between the substrate and the self-assembled film as it was shown by the angular distribution data. They suggest a better ordering on Au single crystals than on gold-coated silicon substrates and particularly better ordering on Au(111) in comparison to Au(100). HREEL spectroscopy is thus a useful approach to access information pertaining to the structure and order of organic ultrathin films.

Acknowledgment. A.-S. D. expresses her gratitude to FRIA (Fonds pour la formation à la Recherche dans l'Industrie et l'Agriculture) for the financial support. Part of this work has been sponsored by the "Région Wallonne" research convention 3119. We thank Dr. Chantal Grégoire and Dr. Petra Rudolf for their interest, suggestions, and many useful discussions.

References and Notes

(1) Di Nardo, N. J.; Demuth, J. E.; Clarke, T. C. *J. Chem. Phys.* **1986**, *85*, 6739.
(2) Pireaux, J.-J.; Thiry, P. A.; Caudano, R.; Pfluger, P. J. *J. Chem. Phys.* **1986**, *84*, 6452.
(3) Wandass, J. H.; Gardella, J. A. *Surf. Sci.* **1985**, *150*, L107.
(4) Wandass, J. H.; Gardella, J. A. *Langmuir* **1986**, *2*, 543.
(5) Wandass, J. H.; Gardella, J. A. *Langmuir* **1987**, *3*, 183.
(6) Rei Vilar, M.; Schott, M.; Pireaux, J.-J.; Grégoire, C.; Caudano, R.; Lapp, A.; da Silva, J. L.; Botelho do Rego, A. M. *Surf. Sci.* **1989**, *211/212*, 782.
(7) Gardella, J. A.; Pireaux, J.-J. *J. Anal. Chem.* **1990**, *62*, 645.
(8) Pireaux, J.-J.; Thiry, P. A.; Sporken, R.; Caudano, R. *Surf. Interface Anal.* **1990**, *15*, 189.
(9) Apai, G. J.; McKenna, W. P. *Langmuir* **1991**, *7*, 2266.
(10) McKenna, W. P.; Apai G. J. *J. Phys. Chem.* **1992**, *96*, 5902.
(11) Yu, L.-M.; Hevesi, K.; Han, B.-Y.; Pireaux, J.-J.; Thiry, P. A.; Caudano, R.; Lambin, P. *Surf. Rev. Lett.* **1995**, *2*, 705.
(12) Yu, L.-M.; Han, B.-Y.; Hevesi, K.; Rudolf, P.; Gensterblum, G.; Thiry, P. A.; Pireaux, J.-J.; Caudano, R.; Lambin, P. *Surf. Rev. Lett.* **1995**, *2*, 557.
(13) Apai, G.; McKenna, W. P. *J. Phys. Chem.* **1994**, *98*, 9735.
(14) Arfa, M. B.; Edard, F.; Tronc, M. *Chem. Phys. Lett.* **1990**, *167*, 602.
(15) Thiry, P. A.; Liehr, M.; Pireaux, J.-J.; Caudano, R. *Phys. Scripta* **1987**, *35*, 368.
(16) (a) Lucas, A. A.; Sunjic, M. *Surf. Sci.* **1972**, *32*, 439. (b) Lucas, A. A.; Sunjic, M. *Prog. Surf. Sci.* **1972**, *2*, 75.
(17) Tong, S. Y.; Li, C. H.; Mills, D. L. *Phys. Rev. Lett.* **1980**, *44*, 407.
(18) Palmer, R. E.; Rous, P. J. *Rev. Mod. Phys.* **1992**, *62*, 383.
(19) Bain, C. D.; Troughton, E. B.; Tao, Y. T.; Evall, J.; Whitesides, G. M.; Nuzzo, R. G. *J. Am. Chem. Soc.* **1989**, *11*, 321.
(20) Ulman, A. *An Introduction to Ultrathin Organic Films-From Langmuir Blodgett to Self-Assembly*; Academic Press: New York, 1991.
(21) Golan, Y.; Margulis, L.; Rubinstein, I. *Surf. Sci.* **1992**, *264*, 312.
(22) Ron, H.; Rubinstein, I. *Langmuir* **1994**, *10*, 4566.
(23) Duwez, A.-S.; Riga, J.; Han, B. Y.; Delhalle, J. *J. Electron Spectrosc. Relat. Phenom.* **1996**, *81*, 55.
(24) Duwez, A.-S.; Di Paolo, S.; Ghijsen, J.; Riga, J.; Deleuze, M.; Delhalle, J. *J. Phys. Chem. B* **1997**, *101*, 884.
(25) Duwez, A.-S. Ph. D Thesis, FUNDP Namur, 1997.
(26) Nuzzo, R. G.; Zegarski, B. R.; Dubois, L. H. *J. Am. Chem. Soc.* **1987**, *109*, 733.
(27) Stern, D. A.; Wellner, E.; Salaita, G. N.; Davidson, L.; Lu, F.; Batina, N.; Frank, D. G.; Zapien, D. C.; Walton, N.; Hubbard, A. T. *J. Am. Chem. Soc.* **1988**, *110*, 4885.
(28) Ertl, G.; Küppers, J. *Low Energy Electrons and Surface Chemistry, Monographs in Modern Chemistry*; Verlag Chemie: Weinheim, 1974.
(29) Strong, L.; Whitesides, G. M. *Langmuir* **1988**, *4*, 546.
(30) Poirier, G. E. *Langmuir* **1997**, *13*, 2019.
(31) Touzov, I.; Gorman, C. B. *J. Phys. Chem. B* **1997**, *101*, 5263.
(32) Jones, R. K. *J. Chem. Phys.* **1985**, *82*, 12.
(33) Grégoire, C. Ph. D thesis, FUNDP Namur, 1996.
(34) Dubois, L. H.; Zegarski, B. R.; Nuzzo, R. G. *J. Chem. Phys.* **1993**, *98*, 678.